

WP 0420 Effect of biomass burning on atmospheric chemistry

Content

WP 0420 Effect of biomass burning on atmospheric chemistry.....	1
Content.....	1
Introduction.....	1
Objectives.....	1
Motivation.....	2
Methodology.....	2
Description of the new Fire Assimilation System (FAS)	3
Background	4
The fire detection algorithm of the MODIS instrument	4
The evaluation of PM _{2.5} emission based on Temperature Anomaly (TA) products.....	4
The evaluation of total PM emission based on Fire Radiative Power (FRP) products.....	5
Connecting the FRP emission factors and the land use	6
Cross-calibration of the FAS-TA and FAS - FRP	7
Operational setup of FAS at FMI.....	12
References.....	14

Introduction

Current report presents the outlook of the Fire Assimilation System that has been developed within the scope of ESA-O3SAF, EU-GEMS, EU-MACC, Aca-IS4FIRES, and TEKES-KASTU projects.

Objectives

An overall objective is to provide a scientific basis for near-real-time evaluation of the emission of trace gases and aerosols from the wild fires and assess and forecast their impact to atmospheric chemistry, in particular, to air quality.

To reach that goal, a set of specific objectives includes:

- to review the existing off-line and near-real-time satellite products concerning the detection and evaluation of wild fires

- to refine the models computing the emission amount and speciation from the space-detected wild fires (both hot spots and burnt areas)
- to establish a modeling system, in cooperation with GEMS, capable of forecasting the influence of the biomass burning on the air quality

Motivation

Biomass burning is recognized as one of the major sources of the reactive gases and aerosols in the troposphere, especially in the tropical regions. They also strongly affect air quality in Europe and other highly populated regions during local summer seasons. Finally, large amount of aerosol and its precursors have their impact on climate change.

As of today, several products estimate the amount of the released species but there are no near-real-time assessments. GEMS intends to develop the first guess of the emitted species on the basis of near-real-time satellite observations but there is a strong need for better models and products, to be developed in cooperation with GEMS. Necessity of such developments complementary to the GEMS activity has been stressed at recent GEMS Annual Assembly.

The information on wild-land fires and products built on its basis (first of all, concentration fields for the released atmospheric contaminants) is crucial for forecasting and evaluation of air quality, visibility deterioration and possible health effects in case of severe episodes.

Methodology

There are two main types of remote-sensing information that are suitable for assessing the features and impacts of fires: products based on estimating the burnt areas, and those using the derivatives of observations of surface temperatures, i.e., hot spot counts and fire radiative power (Flemming, 2005).

Most of the present studies are based on the analyses of burnt areas, which are primarily performed on a monthly basis and diagnosed via, for example, albedo changes at specific wavelengths. Examples of the burnt area products are GLOBSCAR from the ATSR instruments (Simon *et al.*, 2004) and Global Burnt Area 2000 (GBA2000) from SPOT-VEGETATION (Tansey *et al.*, 2004). The burnt area estimates are uncertain and, according to Boschetti *et al.* (2004), the difference between GLOBSCAR and GBA2000 can be as large as a factor of two. There are no burnt-area products available in near-real-time (NRT) at present, which allows the utilization of this type of data only in re-analysis studies.

The other type of input data is based on surface temperature observations and their derivatives. Dozier (1981) and Matson and Dozier (1981) showed that using the information from $3.8\mu\text{m}$ and $11\mu\text{m}$ thermal infrared channels one can detect “sub-resolution scale high temperature sources, and to estimate both the temperature and size of such sources”. This bi-spectral method exploits the different sensitivities of the channels to thermal emission. A sensitivity analysis of Giglio & Kendall (2001) has shown that in realistic conditions the random errors in fire temperature and area retrieved using

Dozier's method are $\pm 100\text{K}$ and $\pm 50\%$ at one standard deviation, respectively, for fires occupying a pixel fraction greater than 0.005. The WF ABBA algorithm (Prins *et al*, 2001) builds on the algorithm by Dozier (1981) to retrieve wildfire size and temperature products from the GOES-8 geostationary meteorological satellite operationally in NRT.

The few intercomparison studies made so far for the burnt-area and hot-spot count approaches indicate severe differences between the methods and even between the retrievals based on the same principle (Boschetti *et al*, 2004).

Most methods to convert the fire information to emissions of atmospheric tracers are based on empirical scaling coefficients from the burnt area (models GWEM of Hoelzemann *et al* (2004), FLAMBE of Reid *et al* (2004), INPE/CPTEC of Freitas *et al*, (2005)) or, rarely, from the hot spots (GFED, Van der Werf *et al*, 2003) to fluxes of a mixture of species. The lists of species included in the emission models vary but usually CO_2 , CO and the total mass of aerosols are included, as these are amongst the most important constituents emitted by fires and measured in the atmosphere, thus allowing a direct calibration of a modelling system. More detailed chemical speciation is usually based on the review by Andrea & Merlet (2001, AM01), in which the most widely used emission factors are provided for the main land use types. However, the speciation also depends on the state of the vegetation, which resulted in a wide range of uncertainties of the mean emission factors.

One of the early operational Fire Alarm Systems based on hot-spot satellite information has been developed in Finland in the mid-1990's and is still operational (<https://virpo.fmi.fi/metsapalo>). The system utilizes the products from the AVHRR and AATSR instruments and generates alarm messages for the authorities and fire-fighting services, if an overheated pixel (compared to the neighbouring ones) appears anywhere in Finland. However, the system provides only qualitative information (the appearance of a fire) and does not describe its intensity or the chemical composition of the emissions.

Description of the new Fire Assimilation System (FAS)

The new FAS is based on Level 2 MODIS Collection 4 and 5 Active Fire Products, which are used for the near-real-time and historical evaluation of the emissions from wild-land fires. The FAS information is processed into the emission input for the atmospheric composition modelling system SILAM for a subsequent evaluation of the impact of fires on atmospheric composition and air quality.

The present FAS consists of two parallel branches based on partly independent products: the Temperature Anomaly and Fire Radiative Power. Their algorithms of converting the fire information to the emission fluxes of atmospheric pollutants are described below, starting from the outlines of the corresponding fire products.

Background

The fire detection algorithm of the MODIS instrument

The MODIS fire detection procedure is based on a contextual algorithm of Giglio et al (2003) that exploits the strong emission of mid-infrared radiation from fires (Dozier, 1981; Matson and Dozier, 1981). The algorithm examines each pixel of the MODIS swath and attributes it to one of the following classes: missing data, cloud, water, non-fire, fire, or unknown. For each fire-classified pixel, the procedure attempts to use the neighbouring pixels to estimate the radiometric signal of the pixel, if there would be no fire there. Valid neighbouring pixels are identified in a window centred on the potential fire pixel and used to estimate this background value.

If the characterization of the background is successful, a series of threshold tests are used to confirm the active-fire hypothesis. These search for the characteristic signature of an active fire, in which both the 4 μm brightness temperature and the difference between the 4 and 11 μm brightness temperatures depart substantially from those of the non-fire background. The thresholds are adjusted based on the natural variability of the background. Additional tests are used to eliminate false detections caused by sun glint, desert boundaries, and errors in the water mask. Candidate fire pixels that are not rejected in the course of these tests are assigned with the class of fire. A dedicated effort is needed to separate the wild-land fires from other types of fires, which is done on the basis of the land use reported for the detected fire pixel.

The evaluation of $PM_{2.5}$ emission based on Temperature Anomaly (TA) products

For simple fire-detection purposes, the fire-classified pixel is attributed with the 4- μm brightness temperature T_4 (this channel is the most-representative and least affected by other factors that are not connected with fires). The method is also known as hot-spot counting and the pixel temperature is further referred to in this study as the TA-value.

The simplicity of this product and its operational availability allowed its utilization as a starting point for FAS development. This branch is hereinafter referred to as FAS-TA. The system receives the input from ASCII telegrams that contain the location, the temperature and the detection confidence of the thermal anomalies. This brightness temperature is then multiplied with an empirical coefficient of 6.78 $\text{ton } PM_{2.5} \text{ yr}^{-1} \text{ K}^{-1}$ to yield an emission flux of $PM_{2.5}$. The scaling was obtained for the Western-Russia (mainly) grass-fire episode in 2006 (Saarikoski *et al.* 2007, hereinafter referred as S07). Input data for the calibration were: (i) the MODIS hot-spot counts (temperature anomaly product) collected over an extensive territory in Western Russia (about 1000km x 1000 km) with a resolution of 1 km, (ii) near-surface observations of $PM_{2.5}$ concentrations in Finland, located directly downwind from the fire at the

distances of about 500-600km. These two datasets were related via FAS-TA and dispersion model SILAM, finally yielding the TA emission factor for PM_{2.5}.

The PM_{2.5} emission fluxes can be converted further to total PM, as well as to other species using the factors of Andrea & Merlet (2001, hereinafter referred as AM01).

The advantages of FAS-TA are its simplicity and the near-real-time (NRT) availability of the data via Rapid Response System (with a delay of just a few hours), which allow its fast application. Also, the system is sensitive to small-scale fires. However, the information obtained from the TA value is limited since the algorithm neglects the background temperature of the fire pixels and uses a simple scaling from temperature to emission rate.

The evaluation of total PM emission based on Fire Radiative Power (FRP) products

For more sophisticated reporting, the MODIS product list includes the Fire Radiative Power (FRP, a rate of release of Radiation Energy, FRE) of the fire pixel, based on the empirical formula of Kaufman *et al* (1998):

$$(1) \quad FRP = 4.34 * 10^{-13} (T_4^8 - T_{4b}^8), \text{ [Watt]},$$

where the T_4 , and T_{4b} are the fire and the background (taken from neighbouring pixels) temperatures, respectively, measured at the 4- μm channel. The dependence has been obtained from fitting the actual release of radiative energy from a fire and its apparent temperature at the 4 and 11 μm channels – as observed by the MODIS instrument. The relationship showed good correlation for open moderate-to-strong fires (Kaufman *et al*, 1998). There may be potential difficulties for small fires, as these may be partly overshadowed by trees, appear as low-temperature but strongly emitting smouldering fires, etc.

As TA, the FRP data are included into the level 2 Fire Products (MOD14 for Terra and MYD14 for Aqua satellites) and are available with a comparatively short delay (usually within 1-2 days), which makes it possible to utilise them within the FAS. However, until recently, FRP has not been available via the Rapid Response System that is practically NRT and updated several times a day. This can cause additional delays in case of technical problems at the central processing or distribution sites. Such delays affect the applicability of the FRP product for the needs of the operational monitoring system.

To convert the FRP to emission fluxes we used a similar approach as for TA – a direct conversion of FRP using an empirical scaling to emission rates. In the current FAS it is based on Ichoku & Kaufman (2005, hereinafter referred as IK05) who related the FRP in [W] per pixel to total particulate matter (PM) emission in [kg tPM s^{-1}]. Since the calibration IK05 was obtained by relating the aerosol optical

depth (AOD) with the FRP, the obtained emission factors are valid for total PM instead of PM_{2.5}, which was the reference species for FAS-TA. The mean relation between these PM measures can be evaluated based on AM01: within the fire plume

$$(2) \quad m_{pm2.5} \approx 0.6m_{total\ pm}$$

The relation is approximately valid for all land use types: the changes between the vegetation types are smaller than the uncertainty range within each type (AM01).

The key parameter for FAS-FRP is therefore the emission rate of total PM per unit FRP, i.e. the smoke emission factor C_e [kg tPM J⁻¹]. According to IK05, C_e varies from 0.02-0.06 kg tPM MJ⁻¹ for boreal regions, 0.04-0.08 kg tPM MJ⁻¹ for Africa (mainly savannas and grassland), and 0.08-0.1 kg tPM MJ⁻¹ for Western Russian regions. Since the C_e determination involved a simple estimate of atmospheric transport (based on wind at a constant height and not involving a dispersion model), the authors suggested that the coefficients are probably overestimated by about a factor of 2. Using these estimates as a starting point, we have developed the emission coefficients that are based on actual land-cover information, instead of geographical region.

Connecting the FRP emission factors and the land use

The procedure of linking the FRP products with the land-use was made in three steps with subsequent 4th step verifying the obtained calibration:

1. the LANDSAT land use inventory for Europe with 250m resolution and USGS with 1km grid spacing were aggregated to the map of the vegetation fractionation with 10km resolution. It included only three types of land use: grass and agriculture land, forests, and a mixture of these;
2. for these three types, we assumed the following total-PM emission coefficients: 0.1 kg tPM MJ⁻¹ for forest, 0.05 kg tPM MJ⁻¹ for grass/agriculture lands, and an average of 0.075 kg tPM MJ⁻¹ for mixed areas. These values were deduced from the prevailing land cover in the IK05 domains;
3. these coefficients were adjusted using the fire episodes 1 and 2, for which the actual location of each daily fire pixel was attributed to one of the land cover types. The emission maps were used as input data by the chemical transport model SILAM, which simulated the atmospheric dispersion of the plumes. The results were compared with the MODIS observations of AOD and the coefficients for the corresponding source types were adjusted.
4. Finally, the PM_{2.5} concentrations computed by the SILAM model were compared with observations of the Finnish stations of Helsinki-Kumpula (urban background), Uto (regional background), Virolahti (regional background), Oulu (small city, urban background) and Vaasa (small city, urban background).

The reference dataset used for the calibration was the aerosol optical depth from MODIS, converted to the total column-integrated PM concentrations (an extension of the MODIS AOD product available e.g. via Giovanni framework <http://daac.gsfc.nasa.gov/techlab/giovanni>). This dataset was utilised for setting the numerical values of the emission factors. The reason for using the satellite observations as the main source of information for the calibration of FAS is that the modelled near-surface concentrations are sensitive to the treatment of the boundary layer in the model. In addition, the ground-based observational network is comparatively scarce and there are potential uncertainties due to the limited spatial representativeness of the sites (Galperin & Sofiev, 1994).

We assumed that inside the fire plumes, the AOD was entirely determined by the biomass-burning products. It is partly supported by S07 analysis, as they found that more than 80% of PM_{2.5} during a specific episode in May 2006 was originated from fires. We therefore attributed all systematic discrepancy between the observed and calculated column AOD to errors in the emission rates, and corrected the emission factors accordingly.

The resulting emission coefficients for the European domain are the following: 0.035 kg tPM MJ⁻¹ for forest, 0.018 kg tPM MJ⁻¹ for grassland and agriculture, and 0.026 kg tPM MJ⁻¹ for mixed areas.

Analysis of the PM_{2.5} and PM₁₀ concentrations obtained with the updated emission factors are discussed in the section **Error! Reference source not found.**

Cross-calibration of the FAS-TA and FAS - FRP

The FRP is physically a better grounded quantity than TA for the determination of the fire emissions: the release of radiative energy is indeed approximately proportional to the number of carbon atoms oxidised per second. Compared to that, the dependence of the brightness temperature on the fire intensity is much less straightforward. It is also more affected by factors that are not directly associated with the fires per se (such as the meteorological ones). Consequently, the TA value should be less sensitive to the fire intensity and, consequently, should have a weaker connection to the emission.

Figure 1 illustrates these differences using the European fires in 2006 as an example. Both panels include all the fires recorded during 2006 with the marker linear dimension proportional to TA (left-hand panel) and FRP (right-hand panel). As one can see, the TA mechanism is much less sensitive to the intensity of a single fire; it reports most of them to be approximately the same intensity. The FRP products reflect better the diversity in the magnitude of the fires, but may under-predict the small fires, many of which are presented on the map as very small dots.

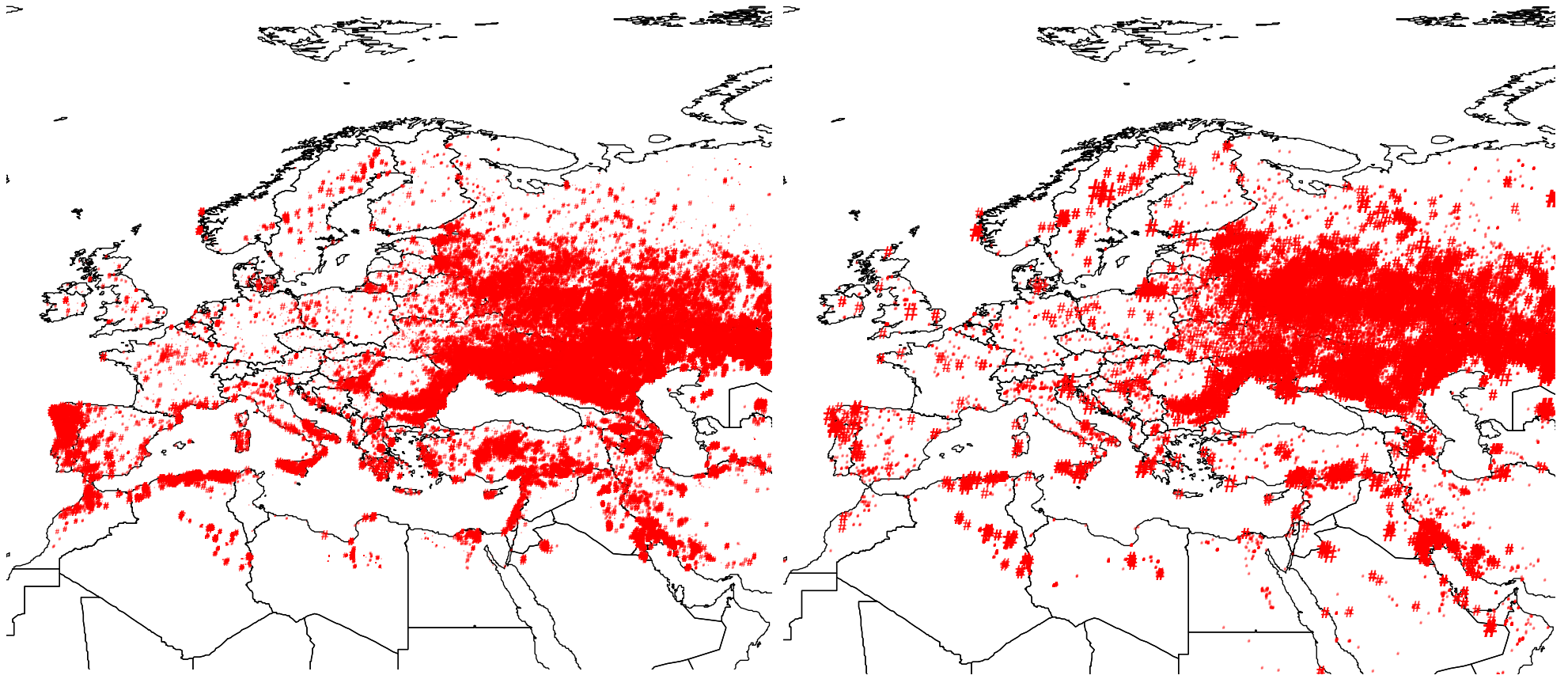


Figure 1. TA- (left-hand panel) and FRP- (right-hand panel) characteristics of the fires in August, 2006. All observed fires are presented. The linear sizes of the markers are proportional to the corresponding TA/FRP values.

However, also the FRP methodology has inherent limitations. Firstly, equation (1) is obtained not via rigorous derivations but via empirical fitting to observations, which makes it dependent on the specific characteristics of the measured data. Secondly, it is presently available only from a few instruments. TA, to the opposite, is available from a wide range of instruments and satellites. Thirdly, the 11- μm channel needed for the computations and for distinguishing between the types of burning is noisy. Fourthly, the reliance on neighbouring pixels for evaluating the background temperature of the burning one can lead to problems, especially in the regions with heterogeneous land use or densely located fires occupying several grid cells. Fifthly, the 8th power of temperatures in eq. (1) makes the final estimates sensitive to inherent noise in the temperature observations. Finally, due to the use of a more sophisticated algorithm, the near-real-time availability of FRP from MODIS was worse than that of TA, reported through the Rapid Response System.

Observing small fires is a special problem, where the combined use of both TA and FRP methods can be efficient. The differences of the 8th powers of temperatures become uncertain, when the burning-pixel and background brightness temperatures approach each other. For such cases, also the chemical composition and the particle size distributions of the emission fluxes are most likely different, compared with the larger scale fires, as the burning becomes less efficient. For smaller fires, the relative fraction of CO₂ is expected to decrease, and the CO, soot and coarse aerosol fractions are expected to increase. As a result, the emissions of coarse aerosols and other trace species related to incomplete combustion processes would be disproportionately larger for small fires, i.e., the FRP and the emission fluxes should be modelled with a less steep temperature dependence than the 8th power. Whether the actual power should be 1, as in TA approach, or something intermediate remains open but it is evident that for small fires, the TA value is closer to the upper estimate of the possible emission rates, and the FRP value closer to the lower one.

It is therefore reasonable to consider the inter-dependence of the predictions of the FAS-TA and FAS-FRP algorithms. For this purpose, we used the dataset of episode 1 (in 2006) and also took into account the split between the three land-use types.

As seen from the scatter plot of FRP against TA values (Figure 2a), there is a functional dependence between these products, with very narrow spread for moderate and strong fires. The noticeable scatter of data for small fires was to be expected. Indeed, besides the above-mentioned methodological difficulties in case of small fires, the TA method does not allow for the background temperature, which becomes comparable with the actual temperature of the pixel if the fire-induced heat release is small. However, the segmentation of the data in terms of the land use types significantly improves the correlation, even for small fires (Figure 2a,b).

The strong connection between FRP and TA and the small scatter allow polynomial fitting of TA to FRP (Figure 2b), which appears valid for all land-use types:

$$(3) \quad FRP = 8.3338 * 10^{-5} * TA^3 - 6.11707 * 10^{-2} * TA^2 + 14.8674 * TA - 1150.92$$

where TA is in [K] and FRP is in [MW].

The relation between the observed FRP and the FRP computed from TA using eq (3) is practically linear, with the regression slope deviating from unity by ~2% and the correlation coefficient of ~0.94 for all land use types. Hence, the values of TA can be converted to FRP with a good accuracy, if the latter ones are unavailable or doubtful.

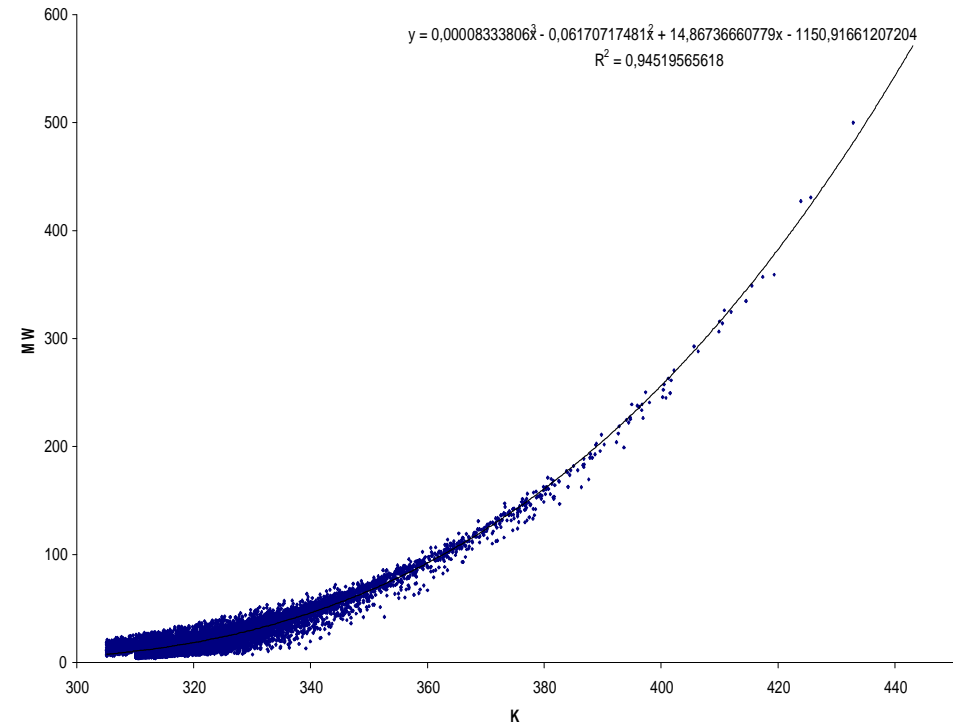
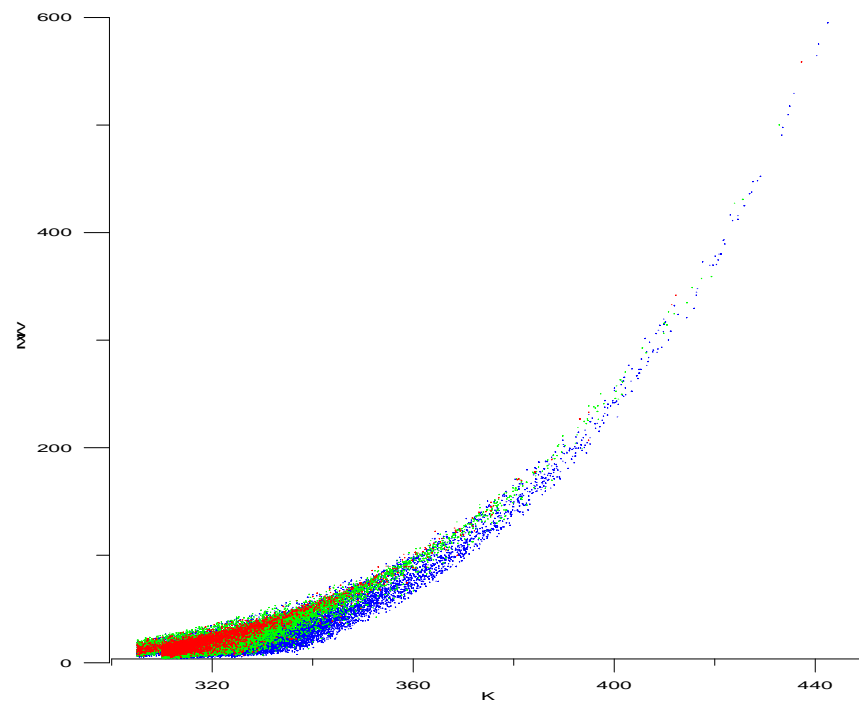


Figure 2. Left-hand panel: The relation between the brightness temperatures, [K] from 21-st band of MODIS (horizontal axis) and FRP for the same fire pixel from MOD14 fire product [MW per pixel area] (vertical axis). Colours of the dots correspond to the land cover types (red – forest, green - mixed forest and grass, blue – grass only). Right-hand-panel: the land-use-independent fitting equation (3) and the forest-fires data sub-set.

Operational setup of FAS at FMI

The current section outlines the implementation of the FAS at Finnish Meteorological Institute and its connections with the air quality modelling. The implementation required solutions of several problems whose detailed descriptions are out of the scope of the current paper. Therefore, the presented outlines aim only at a general outlook, which is relevant for interpreting the FAS application and evaluation results shown in the next sections.

The operational FAS setup includes both TA- and FRP- based branches constructed in a complementary way. For the periods when both TA and FRP are available, the branches are kept independent. Each uses its own linear scaling to emissions of PM_{2.5} and total PM, respectively, which are then scaled to a full list of chemicals according to AM01. For days, in which the FRP data are either unreliable or do not exist, the system converts TA to FRP using the fitting equation (3). This FRP substitution is treated the same way as the original FRP: scaled to total PM emissions and then to the fluxes of other species.

Atmospheric composition forecasts require also forecasts of the evolution of the fires. Presently, these are based on the persistency assumption: the observed fires are assumed to continue for the whole forecasting period (48 hours) with a constant mean intensity equal to the latest recorded level. This simple assumption nevertheless qualitatively reflects two important features: fires that are observed at some moment will continue burning at least several more hours – even in case of a fire brigade intervention. Secondly, even an extinguished fire keeps smouldering for some hours or days; it is therefore still a source of pollutants (clearly, with a different emission rate).

A significant challenge for the current FAS algorithm is the modelling of the diurnal variation of the fire intensity. The main source of information – the MODIS instrument onboard of Aqua and Terra satellites – can provide only 2-4 values per day per place and only during daytime. This is evidently insufficient for the quantitative representation of the diurnal variation. Therefore, we assumed a conservative diurnal variation, same for all types of vegetation and regions, which suggests day-time emission intensity to be 25% higher than the daily-mean level while the night-time emission is 25% lower (Saarikoski *et al*, 2007). The actual variation is probably larger and depends on land-use and meteorology (e.g., Beck & Trevitt, 1989, Beck *et al*, 2001); however, the up-to-date available information on the diurnal variation of the fires is scarce.

The fire-induced PM emission obtained from each FAS branch is merged with other pollution sources taken into account by the SILAM model dispersion simulations – as maps of gridded daily-

mean emission rates with superimposed fixed diurnal cycle. The extension of PM emission to other species used the AM01 factors. We assumed that the following admixture of gaseous species is emitted in addition to PM: 94% of CO, 1.3% of HCHO, 2.9% of NO_x as NO₂, 1.4% of NH₃, and 0.4% of SO₂ (mass fractions as species). The gaseous emission flux is assumed to be 7.9 times larger than the particulate mass flux. These fractions are assumed to be valid for all European land use types. An effort is made to avoid double-counting of the secondary PM. The FAS calibration against MODIS AOD reports all the secondary aerosols as primary emission. A potential way to reduce this effect is to consider the calibration as close as possible to the fires themselves, so that the transport time is short and production of secondary aerosols is limited. That procedure, however, is prone to other uncertainties. The above mentioned regional-scale calibration, having less noise due to spatial and temporal averaging, over-estimates the primary PM emission due to misinterpreting the secondary aerosols as primary ones. According to SILAM chemical simulations, this typically amounts to ~20% of the total aerosol mass.

The SILAM modelling system (Sofiev *et al.*, 2006, 2008) currently includes both Lagrangian and Eulerian dynamic kernels. It takes into account up to 8 different types of the transported species including size-segregated aerosol, sulphur and nitrogen oxides and some VOCs. Operationally, it is used to predict sulphur and nitrogen oxides, ammonium, some hydrocarbons, ozone, sea salt, fine and coarse primary anthropogenic aerosols PM_{2.5} and PM₁₀, as well as biogenic primary aerosols, such as pollen. Other compounds are utilised only in research applications. The current study is based only on the Eulerian-kernel computations with the SILAM v.4.5.1.

Injection height for all fires is prescribed. According to available literature data (Trentmann *et al.*, 2006, Freitas *et al.*, 2007, Zilitinkevich *et al.*, 2006, Labonne *et al.*, 2007, Mazzoni *et al.*, 2007, Kahn *et al.*, 2008, etc), simulations with the BUOYANT plume-rise model (Nikmo *et al.*, 1999), the US fire injection height archive derived from MISR observations over the US (Mazzoni *et al.*, 2007) the plumes from small or moderate fires rarely rise higher than twice the height of the boundary layer H_{ABL} being in most cases confined within 0.5-1 of H_{ABL} , especially if it is deep. For the European fires we therefore assumed simply that 50% of the emissions are injected in the lowest 200 m, and the rest is homogeneously distributed from 200m up to 1km.

The study of the injection height from the fires continues and more accurate evaluation is expected within the scope of O3SAF.

References

- Andreae, M.O., P. Merlet, P. (2001) Emission of trace gases and aerosols from biomass burning,” *Global Biogeochem. Cycles*, vol. 15, pp. 955–966,
- Beck, J.A, Alexander, M.E., Harvey, S. D., Beaver, A. K. (2001) Forecasting diurnal variation in fire intensity for use in wildland fire management applications. *Proc. of Forth Symposium on Fire and Forest Meteorology*, American Met. Soc., http://ams.confex.com/ams/4FIRE/techprogram/meeting_4FIRE.htm
- Beck, J.A. & Trevitt, A.C.F. (1989) Forecasting diurnal variations in meteorological parameters for predicting fire behaviour. *Can. J. For. Res.*, **19**, 791-797.
- Boschetti, L., Eva, H.D., Brivio, P.A., Gregoire, J.M. (2004). Lessons to be learned from the comparison of three satellite-derived biomass burning products. *Geophys. Res. Lett.*, 31, L2150.
- Dozier, J. (1981) A method for satellite identification of surface temperature fields of subpixel resolution. *Rem. Sens. of Environ.* **11**, 221–229.
- Flemming, J. (2005) Emissions for GEMS (biomass burning), HALO discussion paper. Technical report, ECMWF, URL www.ecmwf.int/research/EU_projects/HALO/pdf/paper_HALO_GEMS_emissions.pdf.
- Freitas, S.R., Longo, K.M., Chatfield, R., Latham, D., Silva Dias, M. A. F., Andreae, M.O., Prins, E., Santos, J. C., Gielow, R., and Carvalho, J. A. Jr. (2007) Including the sub-grid scale plume rise of vegetation fires in low resolution atmospheric transport models. *Atmos. Chem. Phys.*, **7**, 3385–3398, www.atmos-chem-phys.net/7/3385/2007/.
- Galperin, M., Sofiev, M. (1994) Errors in the validation of models for long-range transport and critical loads stipulated by stochastic properties of pollution fields. Proc. of EMEP workshop on the Accuracy of Measurements, EMEP/CCC Rep.2/94, pp. 162-179
- Giglio, L. Kendall, J.D. (2001) Application of the dozier retrieval to wildfire characterization: a sensitivity analysis. *Remote Sensing of Environment*, **77(1)**: 34–49.
- Giglio, L. Kendall, J.D., Mack, R. (2003) A multi-year active fire dataset for the tropics derived from the TRMMVIRS. *International J. of Remote Sensing*, **24(22)**: 4505–4525.
- Giglio, L., van der Werf, G. R., Randerson, J. T., Collatz, G. J., and Kasibhatla, P. (2006) Global estimation of burned area using MODIS active fire observations, *Atmos. Chem. Phys.*, **6**, 957-974, [http:// www.atmos-chem-phys.net/6/957/2006](http://www.atmos-chem-phys.net/6/957/2006).
- Hoelzemann, J.J., Schultz, M.G., Brasseur, G.P., Granier, C., Simon, M. (2004) Global wildland fire emission model (GWEM): Evaluating the use of global area burnt satellite data. *Journal of Geophysical Research*, **D109(14)**.

- Ichoku, C., Kaufman, J.Y. (2005) A Method to Derive Smoke Emission Rates From MODIS Fire Radiative Energy Measurements *IEEE Transactions on geoscience and remote sensing*, **43**, No 11.
- Kahn, R.A, Chen, Y., Nelson, D.L., Leung, F-Y., Li, Q., Diner, D.J., Logan, J.A. (2008) Wildfire Smoke Injection Heights – Two Perspectives from Space, *Geophys. Res. Letters*, **35**, L04809, doi:10.1029/2007GL032165,
- Kaufman, Y. J., Justice, C. O., Flynn, L. P., Kendall, J. D., Prins, E. M., Giglio, L. Ward, D. E., Menzel, W. P., Setzer, A. W. (1998) Potential global fire monitoring from EOS-MODIS, *J. Geophys. Res.*, **103**, pp. 32215–32238
- Labonne, M., Bre´on, F.M., Chevallier, F. (2007)Injection height of biomass burning aerosols as seen from a spaceborne lidar. *Geophys. Res. Letters*, **34**, L11806, doi:10.1029/2007GL029311.
- Matson, M., & Dozier, J. (1981). Identification of subresolution high temperature sources using a thermal IR sensor. *Photogramm. Eng. Remote Sens.*, **47**:1311–1318, 1981
- Mazzoni, D., J.A. Logan, D. Diner, R. Kahn, L. Tong, and Q. Li (2007). A data-mining approach to associating MISR smoke plume heights with MODIS fire measurements. *Rem. Sens. Environ.* **107**, 138-148.
- Nikmo, J., Tuovinen, J.P., Kukkonen, J. and Valkama, I., (1999) A hybrid plume model for local-scale atmospheric dispersion. *Atmos. Environ.* **33**, pp. 4389-4399.
- Prins, E., Schmetz, J., Flynn, L., Hillger, D., Feltz, J. (2001) Overview of current and future diurnal active fire monitoring using a suite of international geostationary satellites. In F.J. Ahern, J.G. Goldammer, and C.O. Justice, editors, *Global and Regional Wildfire Monitoring: Current Status and Future Plans*, pp. 145–170. SPB Acad., The Hague, The Netherlands
- Reid, J.S., Prins, E.M., Westphal, D.L., Schmidt, C.C., Richardson, K.A., Christopher, S.A., Eck, T.F., Reid, E.A., Curtis, C.A., Hoffman, J.P. (2004) Real-time monitoring of South American smoke particle emissions and transport using a coupled remote sensing/box-model approach. *Geophys. Res. Lett.*, **31**. L06107.
- Saarikoski, S., Sillanpää, M., Sofiev, M., Timonen, H., Saarnio, K., Teinilä, K., Karppinen, A., Kukkonen, J., Hillamo, R. (2007) Chemical composition of aerosols during a major biomass burning episode over northern Europe in spring 2006: experimental and modelling assessments. *Atmosph. Environ.*, **41**, 3577-3589.
- Simon, M., Plummer, S., Fierens, F., Hoelzemann, J.J., Ariano, O. (2004) Burnt area detection at global scale using ATSR-2: The GLOBSCAR products and their qualification. *J. Geophys. Res. A*, **109**. D14S02.
- Sofiev, M., Galperin, M., Genikhovich, E. (2008) Construction and evaluation of Eulerian dynamic core for the air quality and emergency modeling system SILAM. *NATO Science for piece and security Serties C: Environmental Security. Air pollution modelling and its application*, **XIX**, Borrego, C., Miranda, A.I. (eds.), Springer, pp. 699-701.

- Sofiev, M., Siljamo, P., Ranta, H., Linkosalo, T., Jaeger, S., Jaeger, C., Rasmussen, A., Severova, E., Oksanen, Karppinen, A., Kukkonen, J. (2009b) From Russia to Iceland: an evaluation of a large-scale pollen and chemical air pollution episode during April and May, 2006. *Aerobiological Monographs*, Vol. 1, *in press*.
- Sofiev M., Siljamo, P., Valkama, I., Ilvonen, M., Kukkonen, J. (2006) A dispersion modelling system SILAM and its evaluation against ETEX data. *Atmosph. Environ.* , **40**, 674-685, DOI:10.1016/j.atmosenv.2005.09.069.
- Tansey, K., Gregoire, J.M., Stroppiana, D., Sousa, A., Silva, J., Gereira, J.M.C., Boschetti, L., Maggi, M., Brivio, P.A., Fraser, R., Flasse, S., Ershov, D., Binaghi, E., Graetz, D., Peduzzi, P. (2004) Vegetation burning in the year 2000: Global burned area estimates from SPOT VEGETATION data. *J. Geophys. Res. A*, 109(D14). D14S03.
- Trentmann, J., Luderer, G., Winterrath, T., Fromm, M. D., Servranckx, R., Textor, C., Herzog, M., Graf, H.-F., and Andreae, M. O. (2006) Modeling of biomass smoke injection into the lower stratosphere by a large forest fire (Part I): reference simulation. *Atmos. Chem. Phys.*, **6**, 5247–5260, www.atmos-chem-phys.net/6/5247/2006/.
- van der Werf, G., J.T. Randerson, G.J. Collatz, L. Giglio, P.S. Kasibhatla, A.F. Arellano, S.C. Olsen, and E.S. Kasischke (2004), Continental-scale partitioning of fire emissions during the 1997 to 2001 El Niño/La Niña period, *Science*, **303**, 73-76, 2004
- Zilitinkevich, S. S., Hunt, J. C. R., Esau, I. N., Grachev, A. A., Lalas, D. P., Akylas, E., Tombrou, M., Fairall, C. W., Fernando, H. J. S., Baklanov, A. A., Joffe, S. M. (2006) The influence of large convective eddies on the surface turbulence. *Quarterly Journal of the Royal Meteorological Society* v. 132, pp. 1423-1456.